Laser action in run-away electron preionized diffuse discharges

Alexei N. Panchenko[*, a,b], Mikhail I. Lomaev[a,b], Nikolai A. Panchenko[a], Victor F. Tarasenko[a,b], Alexei I. Suslov[a]
[a]Institute of High Current Electronics, 2/3, Academichesky Avenue, Tomsk, 634055, Russia
[b]Tomsk State University, 36, Lenina Avenue, Tomsk, 634050, Russia

ABSTRACT

Formation features of run-away electron preionized diffuse discharge (REP DD) and REP DD properties in different experimental conditions are studied. It was shown that sufficient uniformity of REP DD allows its application as an excitation source of lasers on different gas mixtures at elevated pressure.

Promising results of REP DD application for development of gas lasers are shown. Stimulated radiation in the IR, visible and UV spectral ranges was obtained in the diffuse discharge. Ultimate efficiency of non-chain HF(DF) chemical and nitrogen lasers on mixtures of SF_6 with $H_2(D_2)$ and N_2 was achieved. New operation mode of nitrogen laser is demonstrated under REP DD excitation. Kinetic model of the REP DD in mixtures of nitrogen with SF_6 is developed allowing to predict the radiation parameters of nitrogen laser at λ = 337,1 nm. Long-pulse operation of rare gas halide lasers was achieved.

Keywords: run-away electron preionized diffuse discharge (REP DD), REP DD properties, efficient gas lasers

1. INTRODUCTION

Formation of a self-sustained volume discharge in high-pressure gas mixtures is main requirement for development of efficient gas lasers. Now it is generally recognized that properly shaped electrodes with no strong edge effects, certain preionization level from different preionization sources (VUV radiation, x-rays, electron beam and so on), over-voltage pulse with short rise-time applied to a laser gap are necessary for formation of spatially homogeneous pulsed avalanche discharges at high gas pressures [1-4]. It is assumed in[1-4] that the volume discharge is formed due to overlapping of primary electron avalanches whose sizes have reached a certain critical value while voltage pulses with short rise time allow to avoid low-preionized near cathode region due to drift of ionizing electrons.

Nevertheless, since the late 1960's, it is known a method for formation of quite uniform discharge in various gases at high pressure even without any preionization[5, 6] if one uses a voltage pulses with high amplitude and short rice-time and electrodes producing non-uniform electric field in a gap. Diffuse discharges in atmospheric pressure helium[5], air[6], and SF_6 gases[7] were obtained. It was found that the discharges can emit intense X-radiation[5, 6]and beams of run-away electrons[8]. Then over time studies of these discharges are not performed mainly due to difficulties in development of sub-ns high-voltage generators and complexity of sub-ns pulse measurements.

During recent ten years intensive study of the discharge type named run-away electron preionized volume (diffuse) discharge (REP DD) has been renewed [9-23] and REP DD was found to have a number of unique properties. Specifically, it was shown that the specific input electric power can be as high as ~100 MW per cubic cm[10,11]. Insufficient effect of the voltage pulse polarity on REP DD formation is found in[12-14]. Diffuse discharges were obtained using voltage pulses with rise-time of several units[10] and tens[14] of ns, as well as, using pulses with amplitude of several tens of kV [10,18]. Repetitive REP DD in bursts and continued modes was obtained with pulse repetition rate up to 3 kHz [19-22].

The REP DD plasma can be used as sources of VUV spontaneous radiation [16,17], for cleaning and modification of metal surfaces[23]. In[22, 24-26] the REP DD was used for gas laser excitation. However, at the moment possible applications of REP DD are studied insufficiently.

The main goal of the present work is study the REP DD development and consideration of possibility of the REP DD application for development of efficient gas laser emitting in different spectral regions.

*alexei@loi.hcei.tsc.ru; phone +7 3822 492-392; fax +7 3822 492-410 ; www.hcei..tsc.ru

XII International Conference on Atomic and Molecular Pulsed Lasers, edited by Victor F. Tarasenko, Andrey M. Kabanov, Proc. of SPIE Vol. 9810, 981004 · © 2015 SPIE
CCC code: 0277-786X/15/$18 · doi: 10.1117/12.2218049

2. EXPERIMENTAL EQUIPMENT AND MEASUREMENT PROCEDURE

The discharge characteristics were investigated using three experimental setups. Fig. 1 shows a design of the output part of SLEP-150M generator[27] (set up 1) and discharge chamber of the RADAN-220 generator (set up 2)[28]. Some experiments were performed using SLEP-150 generator (SLEP-150 generator differs from the SLEP-150M in lack of the transmission line).

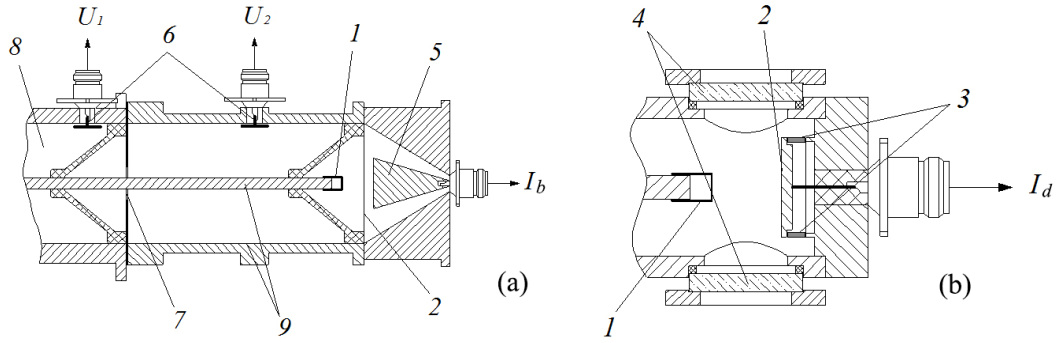

Figure 1. Design of the output part of SLEP-150M generator (a) and discharge chamber of the RADAN-220 generator (b): (*1*) potential electrode, (*2*) plane electrode, (*3*) current shunt, (*4*) windows, (*5*) collector, (*6*) capacitive dividers, (*7*) discharge chopping gap, (*8*) output part of the SLEP-150 generator, and (*9*) transmission line.

The internal diameter of the gas chambers was ~50 mm. Cathode *1* from thin foil tube and a plane anode *2* were used that ensured field amplification near the cathode. Both a 9,5 mm diameter steel sphere (spherical cathode) and a ~6-mm diameter tube made of a 100-μm-thickness steel foil (tubular cathode) were used. The plane anode was made of a brass plate and connected to the chamber casing through a shunt *3*. Anode from a 50-μm Al-Be foil and a grid were used, as well. Collector *5* was installed behind the foil for measurement of a super-short avalanche electron beam (SAEB) characteristic[29]. The discharge glowing was photographed through a grid anode and the current proportional to the displacement current and dynamic displacement current through the gap was measured by the collector, as well. The discharge gap was changed from 0 (short circuit) to 20 mm. Further increase of the gap resulted in the completed surface breakdown on the chamber insulator.

The capacitive voltage dividers were used for voltage pulse measurements while the discharge current I_d was measured by a shunt 3, Fig. 1, assembled from low-impedance chip resistors. The electrical signals from shunt, dividers and collectors were recorded by a 6-GHz-band, 20 GS/s TDS-6604 oscilloscope and a 6-GHz-band, 25 GS/s DPO70604 oscilloscopes.

The RADAN-220 generator (setups 2 and 3) had a wave impedance of 20 Ω and formed a voltage pulse of negative polarity with the amplitude ~250 kV and full width at half maximum (FWHM) of ~2 ns (in case of a matched load) at a discharge gap; the voltage rise-time being equal to ~0,5 ns.

The SLEP-150M and SLEP-150 generators formed the voltage pulses of different polarities with an amplitude on a matched load up to 150 kV and rise-time of ~0,3 ns. The transmission line was filled with oil or air, its impedance was 100 Ω or 140 Ω, respectively. Voltage pulse duration in the line could vary from 1 to 0,1 ns (FWHM) owing to a closing switch installed at the input of the air-filled transmission line. In some experiments, the pulse duration was ~2 ns (FWHM). Fig. 2 shows the waveforms of the voltage pulses with and without the closing switch. The gaps in the switch are 3 and 1 mm. The voltage pulse with ~0,1 ns duration has rise-time of approximately 0,1 ns and the amplitude of ~45 kV, see Fig. 2 (curve 3).

Lasing in various gas mixtures was studied under pumping a RADAN-220 generator connected with laser chamber (set-up 3) shown in Fig.3. The circuitry of the RADAN generator includes a high voltage pulsed forming line (PFL) with capacitance C = 50 pF and oil insulation, which is charged from a Tesla transformer (TT) and than is switched on a load with a commercial two-electrode high-pressure gas spark gap R-49. Two spark gaps with the breakdown voltage of U_1=240±10 kV and U_2=280±10 kV were used in experiments Therewith maximal energy stored in the PFL was E_1=1,56 J (switch No.1) and E_2=2,1 J (switch No.2).

In the experiments the discharge gap d between the blade electrodes 30 cm in length was 1,8 cm. The cavity comprised plane mirrors placed on end walls of the discharge chamber. Its side wall had an additional window for shooting the discharge and detecting the pulses of spontaneous emission. The highly reflecting mirror was made of plates with an

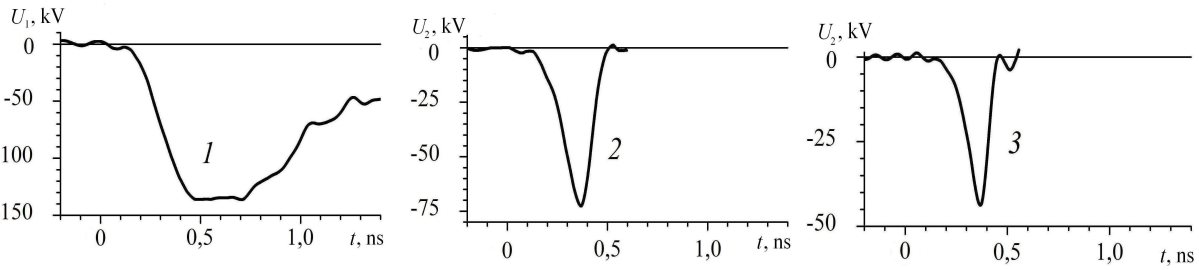

Figure 2. Waveforms of the incident voltage wave, measured by the capacitive dividers at the SLEP-150M output (U_1) and at the transmitting line (U_2): voltage wave falling on the closing switch (*1*), voltage wave after the closing switch with the gap of 3 mm (*2*) and 1 mm (*3*).

aluminum or dielectric coating. Plane-parallel plates made of quartz, CaF_2, KRS-5 (TlBr–40%, TlI–60%), KRS-6 (TlCl–70%, TlBr–30%) crystals or Ge were used as the output mirrors. We also used plane mirrors with dielectric coatings and the reflection coefficients in the UV and visible ranges R = 20 – 100 %. Gas mixtures of SF_6, NF_3, F_2 with H_2, D_2, C_2H_6 and rare gases were used in the experiments.

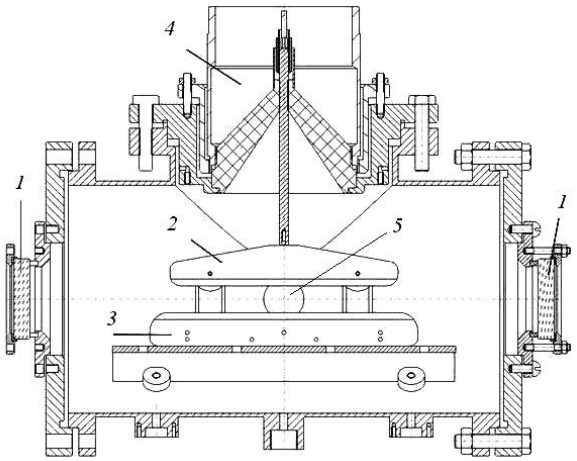

Figure 3. Schematic diagram of the laser pumped by REP DD. (1) mirrors of the laser resonator, (2, 3) blade electrodes, (4) the RADAN-220 pulse generator, (5) side window.

The REP DD current and voltage across the discharge gap were measured with resistive shunt and divider. Visible and UV radiation pulses were detected with a FEK-22SPU photodiode, the IR radiation was detected with a FSG-23 photoresistor. The lasing domain was determined by luminescence on the screen placed on the output mirror. The discharge glow and screen luminescence were photographed by a Sony A100 digital camera. The spectra of radiation in the wavelength range λ = 200 – 850 nm were recorded with a StellarNet EPP2000-C25 spectrometer. Spectra in the range λ = 2,8 – 4,2 mm were measured using an MDR-12 monochromator equipped with a 300 lines/mm grating and FSG-23 photoresistor. The energy of laser radiation was measured by an OPHIR calorimeter with a PE-50BB measuring head. The electrical signals were recorded with a TDS-3054B oscilloscope (0,5 GHz, 5 samples per 1 ns).

3. STUDY OF REP DD FORMATION

As it was pointed out above, in order to form a REP DD, it is necessary to apply high-voltage pulses with ns duration to the gap. Researches of volt-ampere characteristics of a discharge, its spatial form and radiation spectra were carried out using a RADAN-220 and SLEP-150M generators as well as the chambers (Fig. 1). Voltage pulse on a matched load was equal to ~2, ~1, ~0,2, ~0,15 and ~0.1 ns (FWHM). However, real discharge current duration usually exceeded the

generator pulse duration on a matched load due to the sharpening switch inductance and various impedance of the gas discharge plasma during REP DD formation. Fig.4 (a) presents voltage pulses across the gap and discharge current for the ~150 kV incident voltage pulse with duration of ~2 ns[29]. A gas chamber was filled with SF_6 at atmospheric pressure, the discharge being volumetric. It is seen that current in the discharge gap starts at the voltage leading edge and no current oscillation is observed. More than 80% of energy stored in the generator is deposited into the discharge plasma during ~3 ns. The part of the current waveform up to the voltage peak is caused by the displacement current through the "cold" gap. Second peaks on the current and voltage waveforms are related to the pulse reflection from the discharge gap and then from the second end of the generator pulse forming line. Therewith REP DD resistance in SF_6 was measured to be higher than the generator impedance.

In air and nitrogen, as well as in rare gases, the discharge plasma resistance decreases after breakdown essentially faster than in SF_6 and the volume discharge current became oscillating. This situation is shown in Fig.4 (b) where REP DD current in nitrogen at 1 atm for 16 mm gap and RADAN-220 generator is presented. Change of voltage polarity of the electrode with small radius of curvature from negative on positive has negligible effect on the REP DD formation in agreement with the results obtained previously in [11-13]. The beginning of the current pulse from Fig.4 (b) is shown in detail in Fig.4 (c) together with the current of runaway electron beam behind the AlBe foil (a SAEB pulse). The SAEB appears behind the foil approximately 0,6 ns later the voltage pulse start.

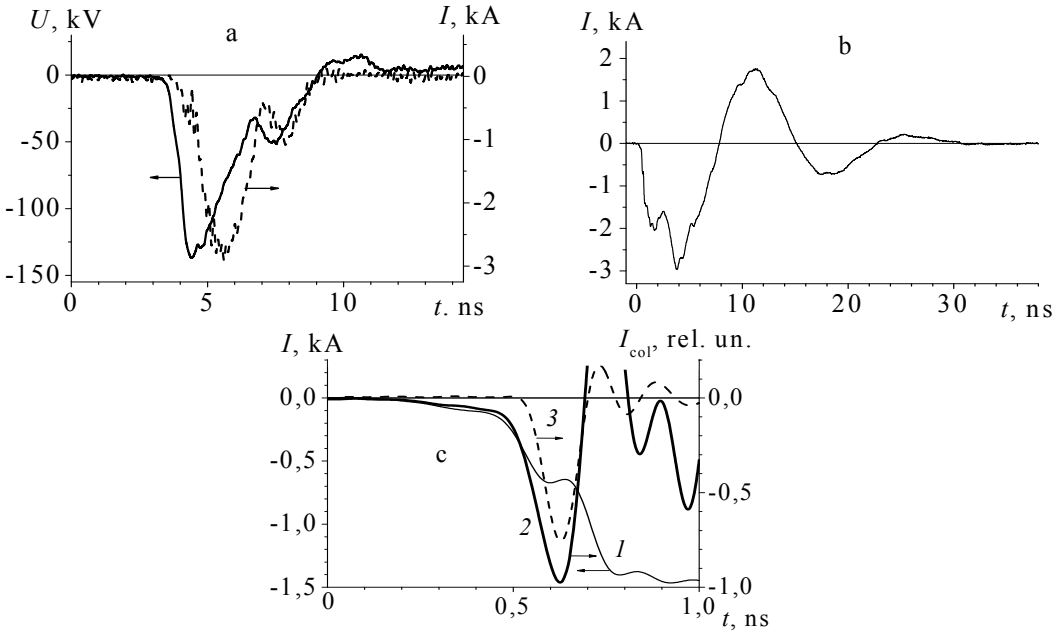

Figure 4. (a) Waveforms of the voltage across the gap U and discharge current I in SF_6 and (b, c) N_2 at p=1 atm; (c) Waveforms of the discharge current registered by a shunt (curve *1*) and SAEB current together with displacement current (curve *2*), electron beam current behind an AlBe foil for maximal oscilloscope time resolution (curve *3*), RADAN-220 generator, gap is 16 mm, curves *1*, *2*, *3* are synchronized in time.

Photographs of the discharge glowing for negative pulse polarity obtained using setups 1 and 2 are presented in Figs.5, 6, 7, respectively. Bright spots are usually seen only on a cathode (C), see Fig.5 (a, b, c), Fig.6 and Fig.7. Pressure increase results in decrease of cross-section of a bright glow discharge region, see Fig.5 (c). In comparatively long gaps the discharge in atmospheric pressure nitrogen, air, SF_6 and other gases was volumetric with the longest voltage pulse durations (~2 ns on a matched load) and its maximal amplitudes (~250 kV). Probability of the discharge contraction is increased for longer voltage pulse duration and its rise-time, higher gas pressure and (or) shorter discharge gaps. Note that in the case of high specific input energy (~1 J/cm^3) from RADAN-220 generator, REP DD transformation into a spark began at the gas pressures of ~0,1 atm.

It is easy to form a REP DD at high pressures in light gases such as He, H_2 and Ne. For instance, diffuse discharge was obtained in He at a pressure up to 15 atm using RADAN-220 generator. Comparing the discharge characteristics in nitrogen and air, one can see that discharge contraction in air is observed earlier than in N_2. As it is seen from Fig.5 (a)

brighter channel appears on the diffuse discharge background in atmospheric air, while discharge glowing maintains its diffuse form in N_2 even at a pressure of 3 atm. When the gap was decreased to 4 mm the discharge

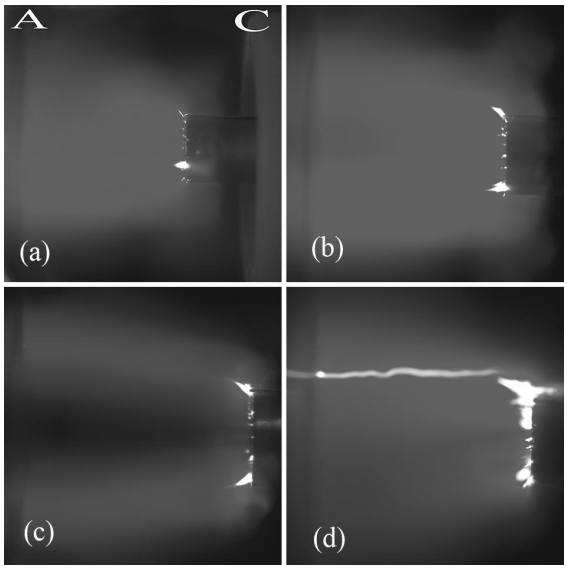

Figure 5. REP DD view in N_2 (a, b, c) and air (d) for the discharge gap 14 mm, RADAN-220 is used, pressure is 0,5 (a), 1 (b, d), and 3 (c) atm.

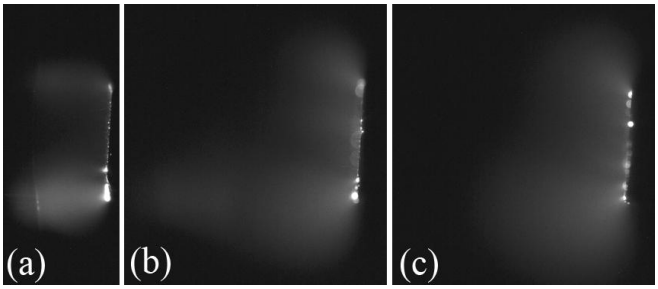

Figure 6. REP DD view in atmospheric air for the discharge gap of 4 (a), 12 (b), and 16 (c) mm, SLEP-150, generator is used.

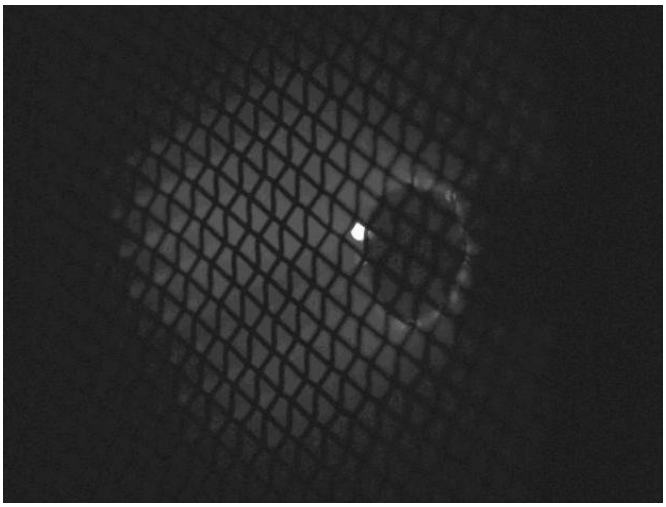

Figure 7. The diffuse discharge glowing in atmospheric air, discharge gap is 12 mm, SLEP-150 generator is used.

constriction was observed both in atmospheric pressure SF_6 and nitrogen with RADAN-220 generator. The gap breakdown voltage decreased with gas pressure for these conditions as it follows from Paschen curve. Therewith in constricted discharge the number of current oscillations increases and total discharge current pulse duration increases, see Fig.4 (b).

Shortening of the voltage pulse duration essentially extends the range of experimental conditions wherein diffuse discharge can be formed. Photographs of the discharge glow in air formed by ~0,2 ns voltage pulses in gaps with different length are presented in Fig.6. Discharge constriction in atmospheric air in 4 mm gap was not observed due to the voltage pulse duration shortening. The REP DD had not enough time to be formed at d = 16 mm, and the glowing was observed only near the cathode which corresponded to a pulsed corona discharge. However, cathode spots had

enough time to be formed in this mode. For the voltage pulse duration of ~2 ns (generator analogous to a SLEP-150), REP DD transition into a corona discharge was observed in longer gaps up to 67 mm in[13]. Fig.7 depicts the photograph of the discharge in air for 12 mm gap and ~1 ns pulse duration. The image was obtained under the angle to the gap longitudinal axis. Owing to reduction of the pulse duration from ~2 ns, (see Fig.5 (d)) to ~1 ns (see Fig.7) and lower voltage pulse amplitude (150 kV) the discharge contraction in atmospheric air is not observed in the gap shortened to 12 mm. The discharge in nitrogen at pressure of 2 atm maintains its diffuse form in gaps expanded up to 20 mm with the RADAN-220 generator.

As follows from these experiments, a REP DD is the initial stage of a spark discharge, which appears when long-duration voltage pulses with slow increase are used. In this case a volume stage of the REP DD is usually hard to see due very high radiation intensity of the spark channels.

Voltage pulse waveforms (incident and reflected from the gap), as well as, the discharge current pulses including displacement current at the voltage pulse edges are presented in Fig.8 for a 12 mm gap. It is seen, that change in discharge mode is observed when the sub-ns voltage pulses are used. For a voltage pulse shorter 0,2 ns (FWHM), (see Fig.8 (a)) the displacement current is seen during the voltage leading edge. The current pulse waveform shows that the dense plasma fails to be in time for overlapping the gap. The discharge glow under these conditions corresponds to the pulse corona discharge (see Fig.6 (c)). If the voltage pulse is longer 0,2 ns (FWHM), one can see the discharge current increase within 0,3 ns (see Fig.8 (b)) due to further development of ionization processes in the whole discharge gap after

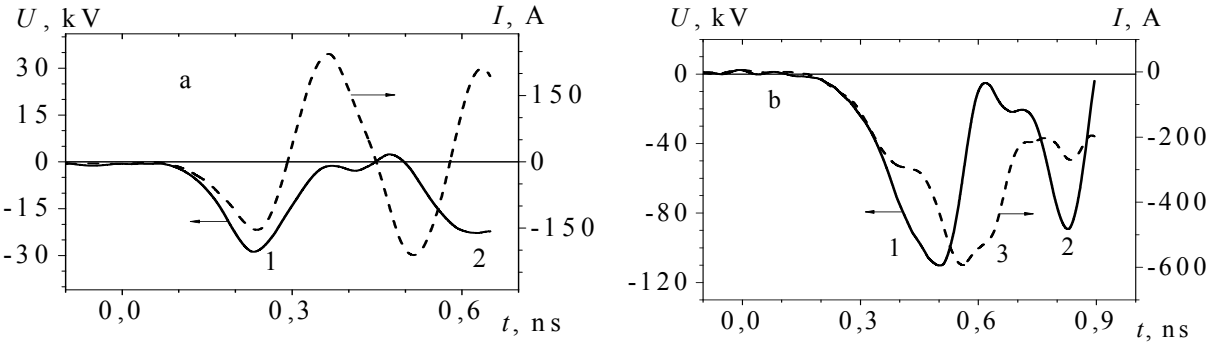

Figure 8. Waveforms of the voltage pulses (incident voltage wave 1, reflected voltage wave 2) and discharge current simultaneously with the displacement current 3, incident voltage pulses duration (FWHM) is 0,1 ns (a) and 0,2 ns (b), SLEP-150M generator, atmospheric air, the gap is 12 mm.

its overlapping by the ionization wave. The gap glow under these conditions corresponds to a REP DD, as shown in Fig.5, Fig.6 (a), and Fig.7. Thus, owing to reduction of the voltage pulse duration and its amplitude, it is possible to realize such discharge mode when the ionization wave front will reach the anode at the moment, when voltage at the gap drops to zero.

Let us consider the REP DD development in laser gap formed between long blade electrodes (set up 3) using N_2 filling as an example[25]. When two blade electrodes were used, diffusive jets originated from both electrodes and overlapped approximately at a distance of 1/3 from the anode. The diameter of the diffusive jets became smaller with increasing N_2 pressure. The gap breakdown voltage depended on the sort and pressure of gas as well as on the rise time of the voltage pulse. As N_2 pressure was changed from 150 Tor to 2 atm, breakdown voltage of the discharge gap increased approximately from 65 to 170 kV.

With lengthening the rise time of the voltage pulse, the diffusive jets became smaller in diameter and spark leaders began to grow from the electrodes. Under these conditions, the spark leaders amounted to several mm in length. The discharge uniformity in the air was lower than in nitrogen. In this case, under similar experimental conditions the diffusive jets in the air were smaller in diameter and the spark leaders began growing at lower pressures. In Ne and H_2 as well as in their mixtures, the discharge uniformity was higher in comparison with discharges in the air and nitrogen. In other gas mixtures under study the REP DD was quite uniform.

Fig. 9 depicts images of the REP DD in nitrogen and laser spots at λ = 337,1 nm obtained at different gas pressure. Since the upper $C^3\Pi_u$ laser level is populated by direct electron impact at values of the parameter E/p>100 V cm^{-1} Tor^{-1}, N_2 laser action occurs in the discharge center where current density is maximal. The highest values of the E/p parameter were achieved for low nitrogen pressures, despite the lowering of the gap breakdown voltage. Specifically, for a N_2

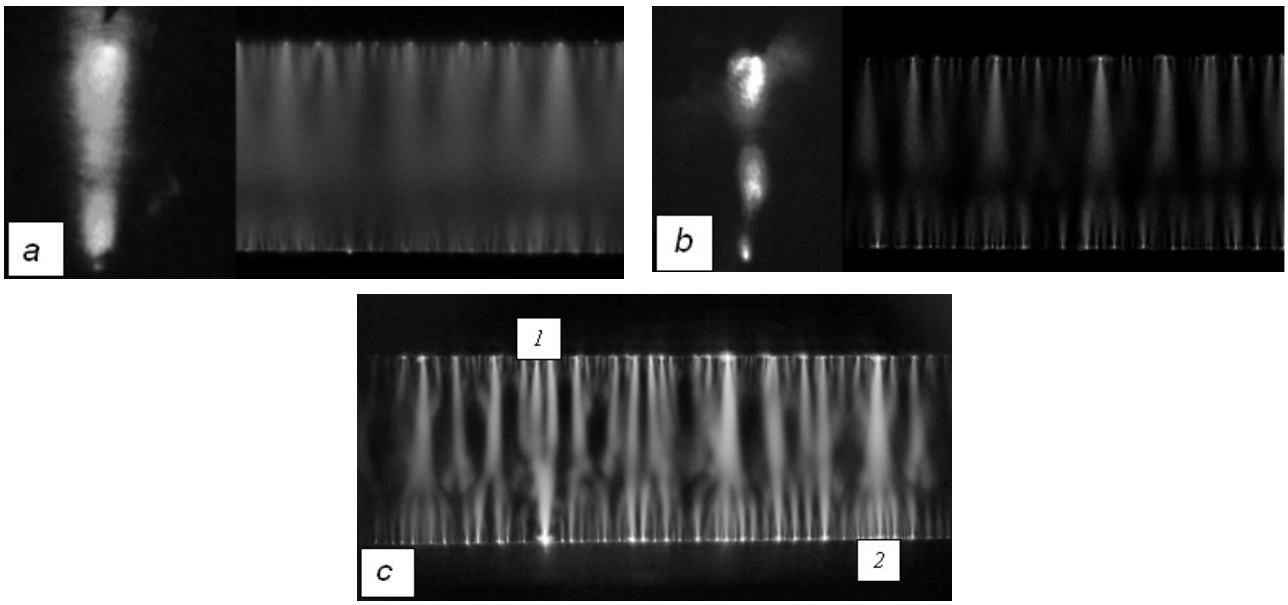

Figure 9. Photographs of discharge glow and laser spot (at the left of Fig.9 (a, b)) for a nitrogen pressure of 0,2 (a) and 2 atm (b, c) and the peak voltage across the gap of 65 (a) and 170 kV (b, c). The discharge gap is d=2 cm. Photograph (c) was taken for a higher responsivity of the camera.

pressure of 150 Tor the average value of the E/p parameter was equal to E/p ~210 V cm^{-1} Tor^{-1}. To determine E/p from oscilloscope traces, the maximum value of the voltage across the gap was divided by the gap width and the gas pressure. As is clear from Fig.9 (a), the highest power density of laser radiation at a low density was recorded from near-electrode regions, where the electric field and the discharge current density are enhanced due to the blade-like shape of the electrodes. In this case, lasing is also observed from the domain adjacent to the side surface of the anode. In the central part of the gap (closer to the anode), the power density of laser radiation becomes lower, which may be attributed both to the lowering of the E/p parameter in the central part of the gap and to its increase above the optimal value. With increasing N_2 pressure, the 'pattern' of laser radiation is substantially changed (see Fig.9 (b)). In the middle of the gap (closer to the anode), for an invariable resonator alignment there appears the third lasing spot. For a N_2 pressure of 2 atm, the average value of the E/p parameter amounts to only 55 V cm^{-1} Tor^{-1} for the maximum voltage across the gap. The threshold of lasing in nitrogen should not be reached for this value of the E/p parameter. In the vicinity of blade electrodes, the electric field is higher than the average one and lasing does take place, as is evident from Fig.9 (b). For low average values of the E/p parameter, the lasing threshold in these regions is attained due to electric field enhancement near both electrodes.

Furthermore, near the electrodes the discharge current densities are maximal, which increases the input power and favors the attainment of the lasing threshold. The emergence of the third laser beam in the discharge gap is attributable only to the enhancement of electric field in this region. To obtain efficient lasing requires, as noted above, that E/p should be no less than E/p = 100 V cm^{-1} Tor^{-1}. Consequently, in the development of gap breakdown there is a phase with a substantial enhancement of the electric field in the gap. As follows from Fig.9, the region of enhanced electric field, which is detected by the emergence of UV lasing in nitrogen, makes its appearance in the interspace between the fronts of ionization waves (diffusive jets). In the motion of the waves towards each other, the greatest enhancement of the electric field at elevated nitrogen pressure should take place in that part of the gap where these waves meet. One can see from the distribution of intensity of laser radiation and the gap glow intensity that lasing takes place in that part of the gap which exhibits a weaker glow (Fig.9 (b)). The photograph of discharge taken under the same conditions for higher camera responsivity is shown in Fig.9 (c). This photograph suggests that the region of lasing is the site of mixing of the diffusive jets, which propagate towards each other from the cathode and the anode. The picture of the 'coalescence' of the diffusive jets varies lengthwise of the electrodes. In particular, in the mixing of three jets directed towards the anode with one jet directed towards the cathode (region 1 in Fig.9 (c)), the brightness of the emission of the latter exhibits an enhancement, and a higher-brightness spot is seen at the anode. A similar picture is seen in another gap region (region

2), but in this case several cathode-directed jets close to one jet directed towards the anode. Furthermore, one can see the intersection of oppositely directed jets at an angle to their propagation direction.

Time delay between the moment the discharge current reaches its peak and the onset of lasing sharply shortens with increasing pressure from 4,5 to 0,5 ns in the pressure interval 0,1 – 0,8 atm and than hardly changed at pressures of 1 – 2 atm. The time characteristics of laser radiation are also testimony to the rise of the electric field in the gap in the propagation of ionization waves.

Thus, our investigations show that there occurs UV lasing on the $C^3\Pi_u \rightarrow B^3\Pi_g$ transition for an average value of parameter $E/p < 60$ V cm^{-1} Tor^{-1} in the gap region where diffusive jets (the fronts of ionization waves) meet at elevated nitrogen pressures. Under these conditions the delay of pulsed lasing from the central gap region was shown to be approximately 1 ns longer than the delay of pulsed lasing from the near-electrode regions. This effect is caused by the enhancement of electric field at the fronts of ionization waves. Similar lasing delay was obtained in mixtures of N_2 with SF_6 and NF_3.

Discharge view in He-F_2 mixture is shown in Fig.10. As in the case of N_2, the discharge consists in diffuse jets, starting from cathode and anode spots. The jets rapidly expand and overlap to the center of gap forming uniform discharge glow. Similar discharge view is observed in all mixtures with fluorine. In contrast to lasing on N_2 (see Fig.9), FI laser spot has a width of 1 cm with a pronounced failure of intensity in the gap center. The lasing threshold on FI transitions is quite low. This means, the central REP DD region high current density is surrounded by a broad low current area.

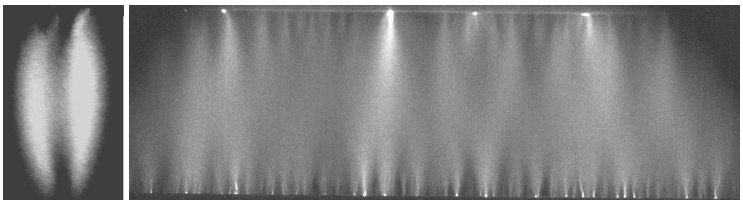

Figure 10. Photographs of FI laser spot (left) and discharge glow (right) in the He:F_2=760:5 Tor gas mixture.

4. GAS LASERS PUMPED BY REP DD

4.1 Nitrogen laser at 337,1 nm

Under pumping N_2 laser by a self-sustained discharge the required value of E/p parameter in the discharge gap can be maintained only several ns. Correspondingly, for efficient laser operation the excitation pulse duration should be shorter than ≈10 ns. Thus parameters of the RADAN generator are optimal for development of nitrogen laser. However, high impedance of the generator requires high discharge resistance which was achieved using additions of SF_6 and NF_3 into gas mixtures. High voltage pulse amplitude allow us to form diffuse discharge without gap preionization in N_2-SF_6 (NF_3) mixtures at pressures up to several atmospheres.

One of the purposes of our study is to construct theoretical model of the discharge laser on nitrogen-electronegative gas mixtures, excited by run-away electron preionized discharge. When simulating the plasma-chemical processes in the volume discharge plasma in N_2-SF_6(NF_3) mixtures and the lasing on transitions in nitrogen, we calculated the following parameters, processes, and objects:

(i) EEDF $fe(E/p, \varepsilon, t)$ in the self-sustained discharge, where E and p are, respectively, the field strength and gas pressure in the discharge gap; ε is the electron energy; and t is time;

(ii) the electron mobility μ_e, temperature T_e, and diffusivity D_e and the rate constants or reactions of electrons with plasma particles;

(iii) kinetic processes involving heavy particles, more than 100 kinetic processes are considered;

(iv) laser radiation;

(vi) pump generator circuit.

All calculation procedures (in the form of individual program blocks) are combined into a self-consistent model, described in details in[30]. Kinetic model of the REP DD allows us to determine optimal gas mixture for achieving

maximal laser efficiency and to predict the radiation parameters of nitrogen laser at λ = 337,1 nm in different gas mixtures of nitrogen with electro-negative additions.

The REP DD model allows us to determine optimal gas mixture for achieving maximal laser efficiency and to predict the radiation parameters of UV nitrogen laser in different gas mixtures of nitrogen with electro-negative additions. Therewith two operation modes of N_2 laser under REP DD excitation were determined from the calculations and in experiments.

Fig.11 illustrates first operation mode. In this case the main part of energy stored in the PFL is deposited into discharge

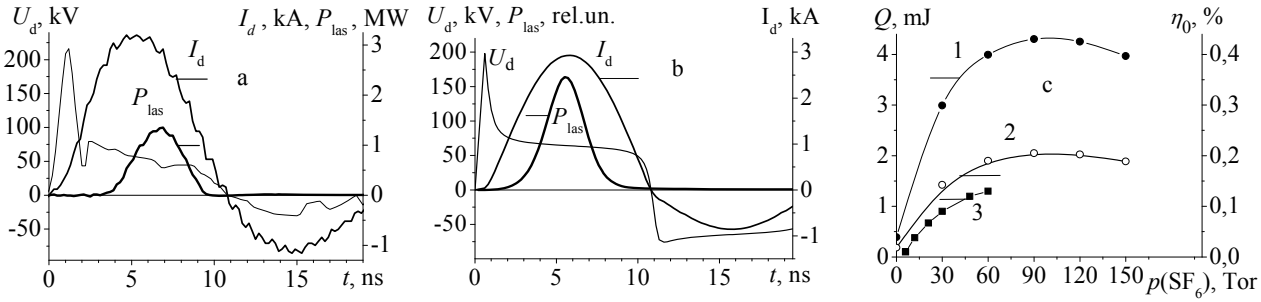

Figure 11. Measured (a) and calculated (b) waveforms of the REP DD current I_d, voltage across the laser gap U_d and laser pulse at λ =337, 1 nm P_{las} in the N_2 : SF_6 = 300 : 90 Tor mixture, N_2 laser energy and efficiency as functions of SF_6 addition in 300 Tor (curves 1, 2) and in 60 Tor (curve 3) N_2 (c). Switch No.2, stored in the PFL line energy E_2=2,1 J.

plasma during 10 ns. Under REP DD pumping the generation domain width was 0,5 cm with the uniform distribution of laser radiation power over the discharge aperture, the peak radiation power reached 1 MW. The maximal energy of the UV radiation was 3,1 mJ with switch No.1 and 4,2 mJ with switch No.2 at the electrical efficiency (with respect to the energy stored in the forming line of the RADAN-220 generator) $\eta_0 \approx$ 0,2 %. Such efficiency is close to the ultimate theoretical value for this type of the laser[31] and to maximal efficiencies obtained experimentally[31, 32]. In the nitrogen mixtures with NF_3 the radiation energy at 337,1 nm was no greater than 0,5 mJ. Besides in that excitation mode weak lasing on first nitrogen system, transition $B^3\Pi_g \rightarrow A^3\Sigma^+_u$ was observed simultaneously with UV lasing[33].

Characteristic feature of second oscillation mode of N_2 laser is two or three radiation peaks during one excitation pulse. This operation mode can be achieved in mixtures of nitrogen with NF_3 and SF_6 under REP DD excitation when the mixture pressure is below ≈100 Tor. The laser output in this case is up to 1,5 mJ, Fig.11 (c).

Two radiation peaks were observed early in[30] when pumping generator with peaking C_1 and storage C_0 capacitors with pulse duration about 100 ns was used. Therewith due to mismatching between the wave resistance of the peaking capacitor circuit and the volume discharge resistance the laser gap voltage and discharge current were modulated by the charge exchange between C_0 and C_1. The amplitude of these modulations is sufficient for periodic formation of the necessary conditions for obtaining population inversion on the $C^3\Pi_u \rightarrow B^3\Pi_g$ transition levels in the laser active medium. As a result, two laser pulses can be formed during one pumping pulse.

In the case of REP DD excitation second and third laser peaks appear during discharge current oscillation. As in the case of pure N_2, initially the lasing emerges at the electrodes. However, delay of the laser pulse appearance in the central discharge part increases to about ~2 ns. The reason for this may be slowing the ionization wave in gas mixtures with SF_6.

The operation mode with several laser peaks is illustrated by Figs. 12–13. The calculations show, that under REP DD excitation electron attachment to electronegative molecules results in further increase of E/p parameter. High attachment rate leads to a rapid drop in the electron number density and recovery of the discharge resistance during current pauses and allows maintaining electric field across the laser gap $E/p > 100$ V cm^{-1} Tor^{-1} during several half-periods of discharge current. Required value of the E/p parameter provides high rate of the upper laser level excitation, maintains population inversion on the $C^3\Pi_u \rightarrow B^3\Pi_g$ transition and results in appearance of successive laser pulses. Therewith in contrast the first operation mode inversion population on $B^3\Pi_g \rightarrow A^3\Sigma^+_u$ transition is not attained. The REP DD is considered to be uniform in the calculations. This result also proves that REP DD in the N_2-SF_6 mixtures maintains its uniformity for a long time.

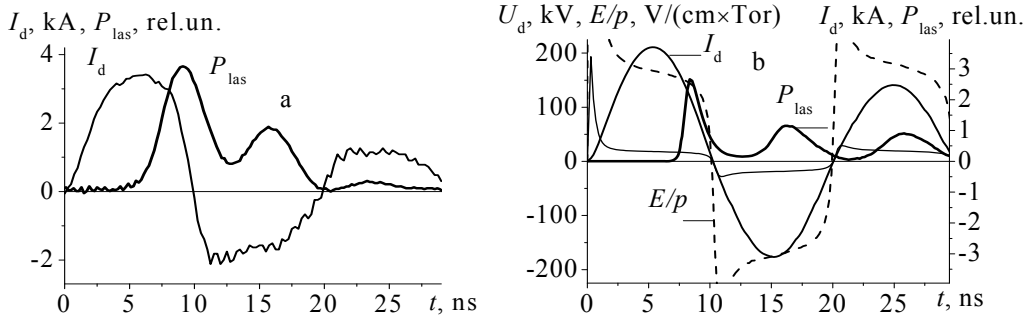

Figure 12. Measured (a) and calculated (b) waveforms of voltage across the laser gap U_d, REP DD current I_d , laser pulses at 337,1 nm P_{las} and temporal dependence of the E/p parameter in mixture $N_2 : SF_6 = 30 : 30$ Tor, E_2=2,1 J.

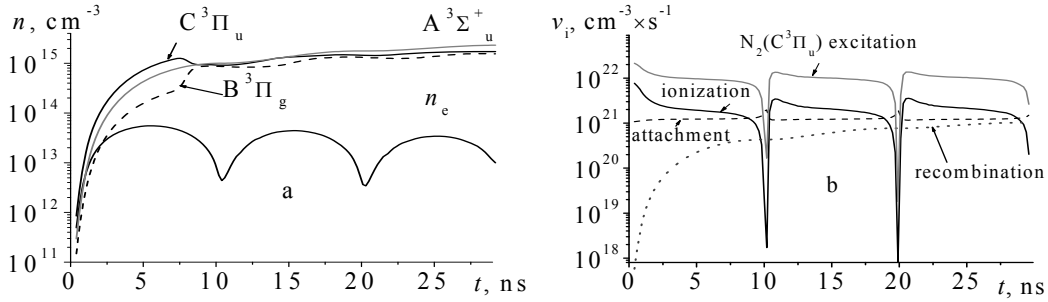

Figure 13. Population densities of nitrogen levels and electrons concentration (a) and rates of different processes in REP DD plasma (b) as functions of time, mixture $N_2 : SF_6 = 30 : 30$ Tor, E_2=2,1 J.

4.2 Non-chain chemical HF(DF) lasers

An interesting feature of SF_6 mixtures with hydrocarbons is the possibility of forming the volume discharge in transverse geometry without preionization[34]. However, volume discharge in the SF_6 mixtures with H_2 or D_2 under conventional excitation regimes is unstable and hence the electrodes are required capable of providing the uniform electrical field in the discharge gap[35], the maximal efficiency of HF(DF) lasers in the mixtures with $H_2(D_2)$ was obtained with short pump pulses (~20 ns)[36].

In our experiments, (see Fig.14) the duration of the REP DD current pulse was about 10 ns without current oscillations.

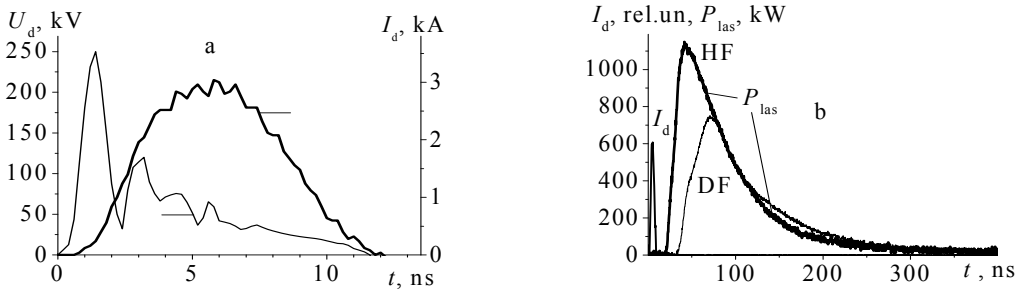

Figure 14. Waveforms of voltage across the laser gap U_d, REP DD current I_d (a, b) and integral pulses of HF(DF) lasers P_{las} (b) in $SF_6 : H_2(D_2) = 8 : 1$ gas mixture, p=300 Tor, switch No.2, E_2=2,1 J.

Estimated from the current and voltage waveforms energy deposed into the laser active medium was E_{in}=1 J. At the volume of the laser active medium of 15 cm^3 such energy deposition corresponds to the specific pumping energy of 65 J/l, which is optimal for a non-chain discharge HF(DF) lasers[33, 35, 37]. The pump power under REP DD excitation reached 20-30 MW/cm^3. The maximal radiation

Maximal output of the HF (110 mJ) and DF lasers (75 mJ) was obtained, similarly to[35, 37], in mixtures with H_2 and D_2. It corresponds to the limiting for discharge HF laser value internal (relative to the energy deposited into the discharge plasma η_{int}) generation efficiency η_{int} = 10%. The obtained DF laser generation efficiency (η_{int} = 7,5%) is also close to

the limiting value for the DF discharge laser (η_{int} = 8%). Similarly to[33, 37], the integral, with respect to spectrum, radiation pulse of non-chain lasers with REP DD pumping had a single peak with peak power over 1 MW and intensive cascade transitions were observed in the generation spectrum.

The number of lasing lines in our experiments attained 16 and 25 in mixtures of SF_6 with H_2 and D_2, respectively. The maximal energy was radiated on the P_1 and P_2 bands of HF and DF molecules. In the case of HF laser the radiation energy distribution over bands was $Q(P_1) : Q(P_2) : Q(P_3)$ = 1 : 0.62 : 0.1. Therewith over 85% of the HF laser output is emitted in intense cascades.

Intense cascade transitions prove the high uniformity of REP DD which provides high uniformity of energy deposition into the active medium. It is knowledge that cascade transitions do not occur in a non-uniform discharge while integral radiation pulse in this case exhibits the well pronounced spike-mode character[37,38]. Cascade transitions increase the efficiency of energy extraction from the active medium of non-chain chemical lasers, because a single excited molecule HF* (v=3) or DF* (v=4), where v is the vibrational quantum number, may emit up to 3–4 photons. The results allow the conclusion that the high homogeneity of a REP DD satisfies the main conditions for volume discharge development in mixtures with SF_6. In this case, due to a high power pumping pulse, the lasing on separate lines stared in 15–20 ns after the discharge gap breakdown with a jitter of 5 ns, which decreases the energy loss for attainment of the lasing threshold. These factors provide for high efficiency of a REP DD pumped non-chain laser.

The high REP DD input power at maximal Q-factor of the cavity resulted in appearance of weak lines in the generation spectrum of HF and DF molecules in the P_4 and P_5 bands with v = 4 and 5, respectively. Lasing in these lines started within ~75 ns after the onset of the discharge current, their intensity was weaker by 2–3 orders of magnitude than that of other lines. The excited molecules HF(DF) with the vibrational quantum number $v > 3$ ($v > 4$) are formed in a "hot" reaction H(D) + F_2, whereas the generation in the $P_4 – P_6$ bands of HF molecules is usually observed under the powerful uniform electron beam pumping[39]. If the mixtures are excited by a conventional transversal self-sustained discharge, the generation threshold in the transitions of HF (DF) molecules with $v > 3 – 4$ is not attained. This fact witnesses a high concentration of molecular fluorine in the REP DD plasma, sufficient for attainment of the lasing threshold.

4.3 FI лазер.

Laser on atomic fluorine (FI) lines in a mixture of He-F_2 emits on several lines in the spectral range from 640 to 775 nm, which could be interesting for a number of applications. Kinetic processes in mixtures of helium with fluorine are part of the kinetics of fluorine-based gas lasers (F_2*, KrF*, ArF* and others) which are still far from being well understood. Therefore the study of FI laser has scientific and practical interest. In addition, in the He-F_2 mixture under short pulse powerful excitation lasing in the VUV at 157 nm can be obtained.

FI laser parameters are shown in Fig.15. A remarkable feature of the atomic fluorine laser is a very broad lasing region.

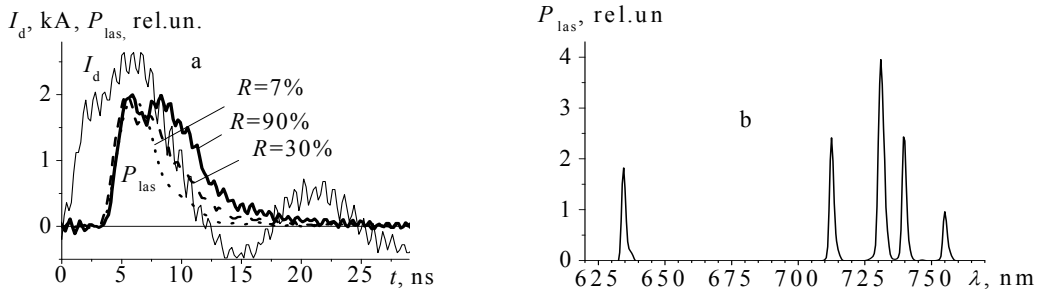

Figure. 15. Waveforms of REP DD current I_d and FI laser pulses P_{las} for different reflectivity R of the output coupler (a) and FI laser spectra (b). Mixture of the He : F_2 = 760 : 4,5 Tor composition is used.

Such a wide aperture lasing is very different from the lasing on N_2 molecules, where the output beam is much narrower (see Figs.9–10). Five lines in the range 634–755 nm are presented in the laser output spectrum. Peak emission power was as high as 10 kW. The laser pulse duration was about 30 ns, which determines duration of volume stage of REP DD, which lasts for a few half-cycles of the current. Discharge view in He-F_2 mixture was shown in Fig.10. Duration of the laser pulses shows only a slight decrease at mixture pressure up to 3 atm. These results suggest the possibility of lasing on F_2 molecules at 157 nm under REP DD excitation.

4.4 Excimer lasers

Fig.16 depicts waveforms of REP DD current, spontaneous emission and laser pulses at 353 and 248 nm. KrF* laser radiation began at the peak of the current pulse. The delay time of XeF* laser pulse was about 5 ns longer due to insufficient cavity Q-factor. Lasing on KrF* and XeF* molecules similarly to[40] lasted during a few half-cycles of the discharge current. It also confirms high REP DD homogeneity in mixtures of rare gases with fluorine. Similar pulse duration was obtained on ArF* molecules in He-Ar-F_2 mixtures. The output of XeF* and KrF* lasers increases with the buffer gas pressure up to 3 atm and reached 10 mJ with peak radiation power about 1 MW.

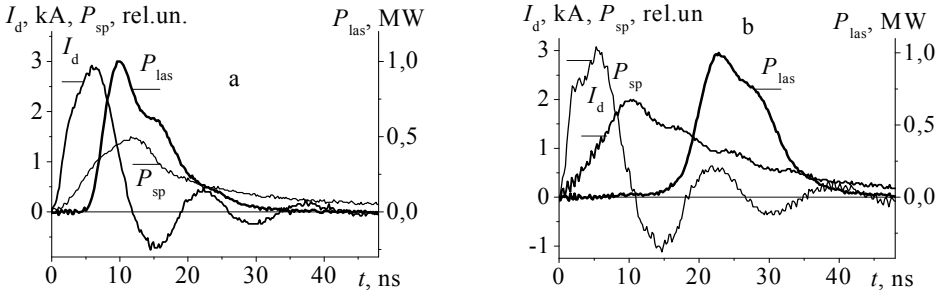

Figure 16. Waveforms of REP DD current (I_d), spontaneous emission (P_{sp}) and laser pulses (P_{las}) on KrF* (a) and XeF* (b) molecules. Gas mixtures He : Kr : F_2 = 3 atm :100 : 5 Tor and He : Xe : F_2 = 3 atm :10 : 5 Tor are used, E_0=2,1 J.

Under REP DD pumping laser action on transitions of helium, neon, argon atoms in the mixtures of inert gases with NF_3 and on nitrogen ion in a He-N_2 mixture was also obtained in visible and UV spectral ranges, as well.

5. CONCLUSIONS

Formation of REP DD and its parameters are studied. It was shown that there occurs UV lasing on N_2 molecules for an average value of parameter $E/p < 60$ V cm^{-1} Tor^{-1} in the gap region where diffusive jets (the fronts of ionization waves) meet at elevated nitrogen pressures. This effect is caused by the enhancement of electric field at the fronts of ionization waves. The pumping regime which involves the enhancement of electric field between counter propagating ionization waves may be employed for obtaining lasing in different gases. Most appropriate for this regime are transitions with a short lifetime of the upper laser level and high excitation energy.

Promising prospects of REP DD application for exciting series of gas lasers are demonstrated. Laser action on molecules N_2, HF and DF with ultimate efficiency was obtained. It was established that the REP DD is most efficient for pumping lasers with the mixtures comprising electro-negative gas SF_6. The addition of SF_6 increases the breakdown voltage in the gaps with electrodes having the shape of blades and makes the pump power higher.

Model of REP DD in N_2-SF_6 mixture is used for simulation of N_2 laser parameters. Novel operation mode of N_2 laser with two and three radiation peaks was demonstrated under pumping by oscillating REP DD.

Efficient laser action on excimer molecules was demonstrated, as well.

Acknowledgments: The work was supported by the Russian Foundation for Basic Researches
(grant No.14-08-00074 a).

REFERENCES

[1] Palmer, A. J., "A physical model on the initiation of atmospheric-pressure glow discharges," Applied Physics Letters 25(3), 138-139 (1974).
[2] Levatter, J.I., Lin, S.C., "Necessary condition for the homogeneous formation of pulsed avalanche discharges at high gas pressures," Journal of Applied Physics 51(1), 210-222 (1980).
[3] Stappaerts, E. A., "A novel analytical design method for discharge laser electrode profiles," Applied Physics Letters, 40(12), 1018-1019 (1982).
[4] Osipov, V. V., "Self-sustained volume discharge," Physics-Uspekhi 43(3), 221-242 (2000)

[5] Noggle, R. C., Krider, E. P., & Wayland, J. R., "A search for X rays from helium and air discharges at atmospheric pressure, "Journal of Applied Physics 39(10), 4746-4748 (1968).
[6] Tarasova, L. V., Khudyakova, L. N., "X rays from pulsed discharges in air," Soviet Physics Technical Physics 14(11), 1148-1151 (1970).
[7] Babich, L. P., Lojko, T. V., "Runaway electrons at high voltage nanosecond discharges in sulfur hexafluoride at pressure of 1 atm," Zh. Tech. Phys. 61(9), 153-155 (1991).
[8] Tarasova, L. V., Khudyakova, L. N., Loiko, T. V., Tsukerman, V. A., "Runaway electrons and X-Ray radiation of the nanosecond pulsed gas discharges at pressures of 0,1–760 Tor," Zh. Tekh. Fiz. 44(5), 564-568 (1974).
[9] Tarasenko, V. F., Orlovskii, V. M., Shunailov, S. A., "Forming of an electron beam and a volume discharge in air at atmospheric pressure," Russian Physics Journal 46(3), 325–327 (2003).
[10] Alekseev, S. B., Gubanov, V. P., Kostyrya, I. D., Orlovskii, V. M., and Tarasenko, V. F., "Pulsed volume discharge in a nonuniform electric field at a high pressure and the short leading edge of a voltage pulse," Quantum Electronics 34(11), 1007-1010 (2011).
[11] Tarasenko, V. F.; Yakovlenko, S. I., "Electron runaway mechanism in dense gases and the production of high-power subnanosecond electron beams," Phys. Usp. 47(9), 887-907 (2004).
[12] Kostyrya, I. D., Tarasenko, V. F., "On the formation of nanosecond volume discharges, subnanosecond runaway electron beams, and x-ray radiation in gases at elevated pressure," Russian Physics Journal 48(12), 1257-1269 (2004).
[13] Kostyrya, I. D., Orlovskii, V. M., Tarasenko, V. F., Tkachev, A. N, Jakovlenko, S. I., "Atmospheric pressure volume discharge without external preionization," Technical Physics Letters 31(6), 457-460 (2005).
[14] Bratchikov, V. B., Gagarinov, K. A., Kostyrya, I.D., Tarasenko, V. F., Tkachev, A. N., Yakovlenko, S. I., "X-ray radiation from the volume discharge in atmospheric-pressure air," Technical Physics 52(7), 856-864 (2007).
[15] Krompholz, H. G., Hatfield, L. L., Neuber, A. A., Kohl, K. P., Chaporro, J. E., Ryu, H., "Phenomenology of subnanosecond gas discharges at pressures below one atmosphere," IEEE Transactions on Plasma Science 34(3), 927-936 (2006).
[16] Baksht, E. Kh., Lomaev, M. I., Rybka, D. V., Tarasenko, V. F., "Emission of a volume nanosecond discharge plasma in xenon, krypton, and argon at high pressures," Quantum Electronics 36(6), 576–580 (2006).
[17] Lomaev, M. I., Mesyats, G. A., Rybka, V. D., Tarasenko, V. F., Baksht, E. Kh., "High-power short-pulse xenon dimer spontaneous radiation source," Quantum Electronics 37(6), 595-596 (2007).
[18] Baksht, E. H., Burachenko, A. G., Lomaev, M. I., Rybka, D. V., Tarasenko, V. F., "Effect of gas pressure on amplitude and duration of electron beam current in a gas-filled diode," Technical Physics 53(12), 93-98 (2008).
[19] Tarasenko, V. F., "Nanosecond discharge in air at atmospheric pressure as an x-ray source with high pulse repetition rates," Applied Physics Letters 88(8), 081501 (2006).
[20] Shao, T., Zhang, Ch., Niu, Z., Yan, P., Tarasenko, V. F., Baksht, E. Kh., Kostyrya, I. D., Shut'ko, Yu. V., "Diffuse discharge, runaway electron, and x-ray in atmospheric pressure air in an inhomogeneous electrical field in repetitive pulsed modes," Applied Physics Letters 98(2), 021503 (2011).
[21] Shao, T., Tarasenko, V. F., Zhang, Ch.; Baksht, E. Kh., Zhang, D., Erofeev, M. V., Ren, Ch., Shut'ko, Yu. V., Yan, P., "Diffuse discharge produced by repetitive nanosecond pulses in open air, nitrogen and helium," Journal of Applied Physics 113(3), 093301 (2013).
[22] Baksht, E. Kh., Burachenko, A. G., Lomaev, M. I., Panchenko, A. N., Tarasenko, V. F. "Repetitively pulsed UV radiation source based on a volume discharge initiated by an avalanche electron beam in nitrogen," Quantum Electronics 45(4), 366–370 (2015).
[23] Shulepov, M. A., Tarasenko, V. F., Goncharenko, I. M., Koval', N. N., Kostyrya, I. D., "Modification of the near–surface layers of a copper foil under the action of a volume gas discharge in air at atmospheric pressure," Technical Physics Letters 34(4), 296-299 (2008).
[24] Baksht, E Kh., Burachenko, A. G., Tarasenko, V. F., "Lasing in nitrogen pumped by a runaway-electron-preionized diffuse discharge," Quantum Electronics 39(12), 1107-1111 (2009).
[25] Tarasenko, V. F., Tel'minov, A. E., Burachenko, A. G., Rybka, D. V., Baksht, E. Kh., Lomaev, M. I., Panchenko, A. N., and Vil'tovskii, P. O., "Lasing from the domain of collision of ionization waves produced due to electric field concentration at electrodes with small radius of curvature," Quantum Electronics 41(12), 1098-1103 (2011).
[26] Vil'tovskii, P. O., Lomaev, M. I., Panchenko, A. N., Panchenko, N. A., Rybka, D. V., Tarasenko V. F., "Lasing in the UV, IR and visible spectral ranges in a runaway-electron-preionized diffuse discharge," Quantum Electronics 43(7), 605-609 (2013).

[27] Tarasenko, V. F., Kostyrya, I. D., Baksht, E. Kh., Rybka, D. V.,"SLEP-150M compact super-short avalanche electron beam accelerator," IEEE Trans. Dielectr. Electr. Insul. 18(4), 1250-1255 (2011).
[28] Mesyats, G. A., Korovin, S. D., Rostov, V. V., Shpak, V. G., and Yalandin M. I., "The RADAN series of compact pulsed power generators and their applications," Proceedings of the IEEE 92(7), 1166-1179 (2004).
[29] Tarasenko, V. F., "Parameters of a supershort avalanche electron beam generated in atmospheric-pressure air," Plasma Physics Repots 37(5), 409-421 (2011).
[30] Panchenko, A. N., Suslov, A. I., Tarasenko, V. F., Konovalov, I. N., and Tel'minov A. E., "Laser on nitrogen-electronegative gas mixtures, pumped by inductive energy storage generator: experiment and theoretical model," Physics of Wave Phenomena 17(4), 251-276 (2009).
[31] Tarasenko, V. F., "Efficiency of a nitrogen UV laser pumped by a self–sustained discharge," Quantum Electronics 31(6), 489-494 (2001).
[32] Iwasaki, C., and Jitsuno, T., "An investigation of the effects of the discharge parameters on the performance of a TEA N_2 laser," IEEE Journal of Quantum Electronics 18(3), 423-427 (1982).
[33] Panchenko, A. N., Lomaev, M. I., Panchenko, N. A., Tarasenko, V. F., Suslov, A. I., "Efficient gas lasers pumped by run-away electron preionized diffuse discharge," Proc. SPIE 9255, 92552V (2015).
[34] Apollonov, V. V., Belevtsev, A. A., Firsov, K. N., Kazantsev, S. Yu., Saifulin, A. V., "Self-initiated volume discharge in mixtures of SF_6 with hydrocarbons to excite nonchain HF lasers," Proc. SPIE 4071, 31-43 (2000).
[35] Panchenko, A. N., and Tarasenko, V. F. "Efficient discharge-pumped non-chain HF and DF lasers," Proc. SPIE 6101, 61011P-1 (2006).
[36] Midorikawa, K., Sumida, S., Sato, Y., Obara, M., Fujioka, T., "Efficient operation of a low-impedance Blumlein discharge initiated HF/DF chemical laser," IEEE J. Quant. Electronics 15(3), 190-194 (1979).
[37] Panchenko, A. N., Orlovsky, V. M., Tarasenko, V. F., "Spectral characteristics of non-chain HF and DF electric–discharge lasers in efficient excitation modes," Quantum Electronics 34(4), 320-324 (2004).
[38] Baranov, V. Yu., Vysikailo, F. I., Dem'yanov, A. V., Malyuta, D. D., Tolstov, V. F., "Parametric investigation of a pulsed non-chain HF laser," Soviet Journal of Quantum Electronics 14(6), 791-795 (1984).
[39] Erofeev, M. V., Orlovskii, V. M., Skakun, V. S., Sosnin, E. A., Tarasenko, V. F., "Efficiency of an H_2–SF_6 laser with electron – beam initiation of chemical reactions," Quantum Electronics 30(6), 486-488 (2000).
[40] Kakizaki, K., Sasaki, Y., Inoue, T., Sakai, Y., "High-repetition-rate (6 kHz) and long-pulse-duration (50 ns) ArF excimer laser for sub-65 nm lithography," Review of Scientific Instruments 77(3), 035109 (2006).